

# Shaping Off-Axis Metallic Membrane Reflectors Using Optimal Boundary Shapes and Inelastic Strains

C.V. White\* M. Dragovan

Jet Propulsion Laboratory  
M/S 157-316  
4800 Oak Grove Drive  
Pasadena, CA 91109  
[christopher.v.white@jpl.nasa.gov](mailto:christopher.v.white@jpl.nasa.gov)  
tel: (818)354-2869

\* Corresponding author

## Introduction

This paper will describe a novel concept for constructing off-axis membrane reflector surfaces. Membrane reflectors have been extensively studied, including investigations into inflated lenticular architectures, shaping by spin casting [4,5,6], shaping using electrostatic forces [2,3], and shaping by evacuating behind a membrane surface stretched between circular or annular-shaped supports [15,1]. The majority of these investigations has considered polymeric membrane materials and material stresses were low. Other researchers have investigated the membrane inflation problem for nonlinear or viscoelastic rubber-like materials undergoing large elastic strains [9,10,12]. Such work has applications in biomechanics and automotive industries.

In contrast to these previous studies, we propose the use of metallic membranes (thin foils) which are initially flat and supported along the boundary then deformed by vacuum into doubly curved surfaces with internal strains well past the material yield point. Once the membrane has been thus shaped, it will largely retain its shape due to locked-in plastic strains, and the vacuum can be either removed or greatly reduced. If a small amount of vacuum is applied, the membrane is greatly stiffened, although its shape is not much altered. Aspects of this idea for air-supported roof structures were investigated as early as 1944 [11].

The basic feasibility of this concept has been experimentally demonstrated by forming a half-meter size rotationally symmetric paraboloid, using both electroformed copper and stainless steel foils. Due to the success of the technique for on-axis symmetric construction, it is of extreme interest to understand the process by which off-axis reflecting surfaces might be constructed. The principle advantage of the off-axis geometry is the possibility of an unobstructed aperture, which provides enhanced performance to the reflector.

If this technique proves feasible for constructing off-axis reflectors, a whole class of cheap, simple and potentially very large reflectors could be made at a fraction of the time and expense required for traditional metal or glass reflectors. Such reflectors would have extremely low areal densities,

easing the loads on the supporting structure and driving down the price of the entire telescope. There are applications for both space-based and ground telescopes, particularly in sub-mm and IR.

## Approach

As with the forming processes cited above, this technique can at best only approximate a parabolic surface. See the following references for some interesting remarks on approximating parabolic surfaces, both on-axis and off-axis [7,8,13,14]. One of the distinguishing features, and one of the challenges of the proposed technique, is the dependence of the ultimate shape on the plastic and residual strain distribution and its associated analytical prediction. Moreover, there is a strong interaction between the shape of the boundary and the shape of the surface in a way that is not well understood yet. As a first phase of our investigation, we cast the problem as one of optimizing the boundary shape in such a way as to minimize the residuals to a target off-axis surface.

Figure 1 shows the geometry associated with an off-axis parabolic surface. A convenient expression for the desired off-axis surface can be found in [8], and is repeated here:

$$z = \frac{1}{\sin^2 \theta} \left[ \cos \theta \sin \theta x + 2 \cos \theta f - \left( -y^2 \sin^2 \theta + 4 \cos^2 \theta \sin \theta x + 4 \cos^2 \theta f^2 \right)^{1/2} \right]$$

The desired surface has the property that the focal point is located outside the edge of the aperture, such that  $f \sin(\theta) \gg \text{aperture}/2$ .

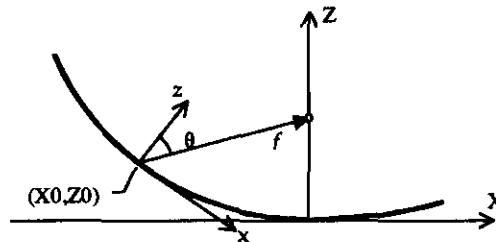


**Figure 1** A portion of the parabolic generator of a rotationally symmetric reflecting surface. The off-axis segment is centered about the point  $(X_0, Z_0)$ , and focuses to a point located distance  $f$  away.

Fully geometric and material nonlinear finite element analysis is used to compute the surface shape for a given pressure. The commercial finite element program LS-DYNA3D is used for the analysis. The nonlinear material model accepts user-defined stress-strain curves and employs a kinematic plasticity model based on von Mises stresses. Deviation of the computed surface from the target surface is expressed as a surface RMS error, which is computed in MATLAB.

The initially flat membrane is assumed to have a rigid boundary whose shape is constrained to belong to a family of mathematical curves. Although we have restricted our attention exclusively

to ellipses so far, any family of curves including circles, ovals, rectangles, etc. could be considered. The parameters that define these curves are naturally the design variables for the optimization. The commercial software LS-OPT, based on the response surface methodology, is used to determine the parameter values that minimize the surface RMS error.

## Results

Stress-strain data were measured for 50-micron thick samples of both electroformed copper foil and Grade 321 stainless steel foil. The results are shown in Figure 2. These experimental results were used to define the material behavior for the finite element simulations. To verify the accuracy of the simulations, an experiment was performed on a 50 cm diameter 321 stainless membrane with a circular boundary. Vacuum was measured with a pressure transducer, and the central deflection was measured with a precision LVDT. The comparison between the measurements and the LS-DYNA3D analysis, shown in Figure 3, confirms the accuracy of the nonlinear finite element analysis. In this case, the FE analysis indicates a maximum strain of 0.14, which is comfortably below the material's failure strain.

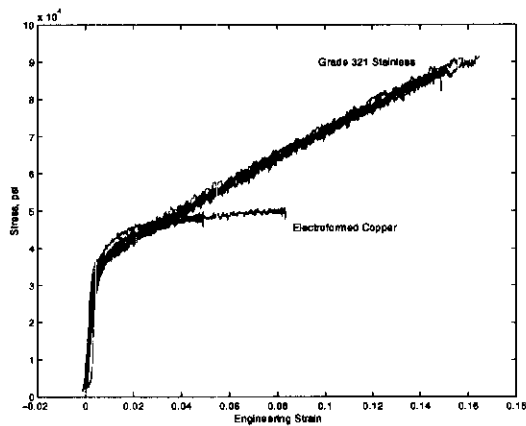


Figure 2 Stress strain measurements for the copper and stainless steel foils. The copper material was tested to failure; the ductility of the stainless exceeded the capabilities of the extensometer.

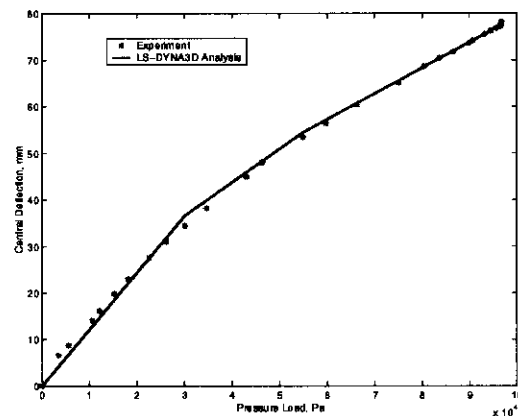


Figure 3 Load-deflection curve for on-axis stainless steel membrane.

For the off-axis geometry, the boundary of the membrane is assumed to belong to the family of asymmetrical ellipses, as depicted in Figure 4. The choice of ellipses is based on judgment alone, but it appears to be a reasonable starting point. Interestingly, the entire family of such ellipses can be generated by independently scaling two semi-circular areas along one of their axes. With reference to Figure 4,  $R$  represents the radius of the semicircles, which becomes the semi-minor axis of the ellipse, and  $scale\_L$  and  $scale\_R$  are the scale factors for the left and right semi-major axes of the ellipse. Thus, with a fixed radius  $R$  of 50cm, the boundary is completely parameterized by  $scale\_L$  and  $scale\_R$ , which become design variables in the optimization.

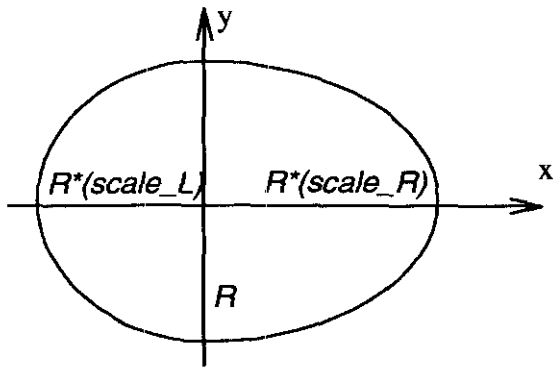


Figure 4 An asymmetrical elliptical boundary can be described by equal semi-minor axes and different semi-major axes.

DRDF ASYMMETRICAL ELLIPTICAL MEMBRANE  
Time = 0

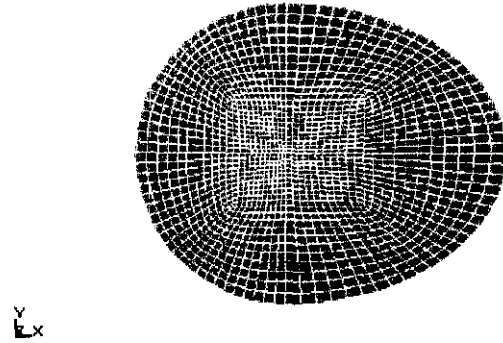


Figure 5 Little mesh distortion results when reasonable scale factors are applied. In this figure,  $scale\_L = 1.0$ , and  $scale\_R = 1.45$ .

It is a simple matter to modify the finite element geometry for each instance of the parameters by applying the scale factors  $scale\_L$  and  $scale\_R$  to the x-coordinates of all nodes of two meshed semicircular areas. This step is performed automatically in LS-OPT without user intervention. An example of a scaled mesh is shown in Figure 5.

Maximum applied pressure is added to  $scale\_L$  and  $scale\_R$  for a total of three design variables, and the optimization is run with the objective of minimizing residual error to a target surface, which is specified in terms of  $(f, \theta)$  per Figure 1. Representative results of the optimization process are shown in Figure 6 through Figure 8. It is seen from Figure 7 that the RMS error is in the neighborhood of  $400 \mu\text{m}$ , with a corresponding pressure of roughly  $\frac{1}{2}$  atm.

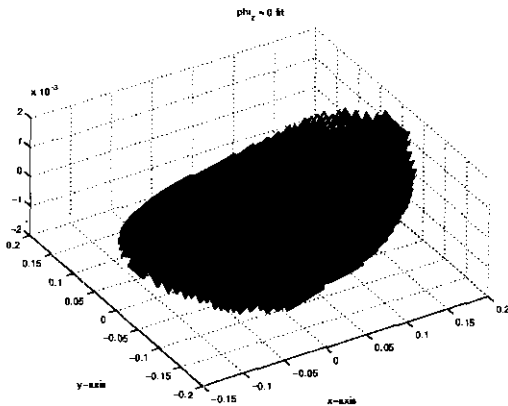


Figure 6 For any boundary shape and pressure level, a surface plot of the residuals quickly shows the spatial distribution of the errors.

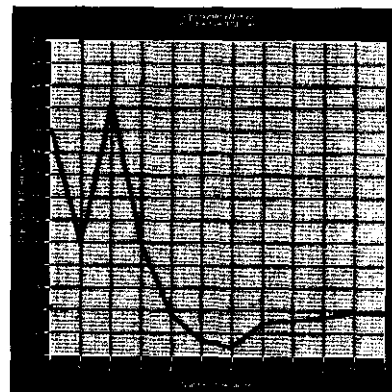
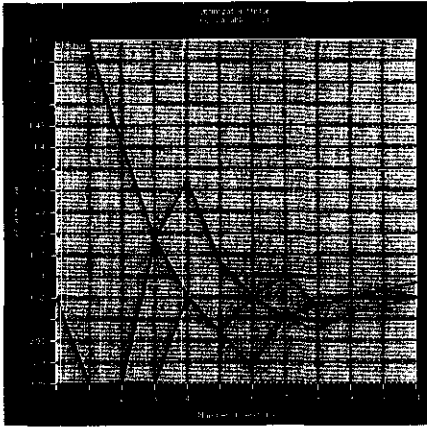


Figure 7 Evolution of the RMS of the residual surface (the objective function),  $\mu\text{m}$ , as the iterations proceed. The individual points represent computed values; the solid black line indicates the predictions by the response surface.



**Figure 8 Evolution of the scale\_L design variable and its upper and lower bounds versus iteration number.**

## Conclusions

The problem of forming off-axis parabolic reflectors by inducing inelastic strains in metallic foils has been successfully cast as one of minimizing surface figure errors by choice of the design variables boundary shape and maximum applied pressure. Software tools necessary for such an investigation -- the nonlinear finite element solver, the custom programs to compute surface residuals, and the optimization engine -- have been assembled and successfully integrated.

For the specific family of boundary shapes so far investigated, namely asymmetric ellipses, surface figure errors of nearly 400  $\mu\text{m}$  are indicated. It is anticipated that more extensive analysis will provide insights that can lead us to more precise reflector designs. The final publication in early 2004 will include the results of this additional work.

## References

1. Waddell, P. '*Development of a Stretchable Concave Imaging Membrane Mirror of Variable Focus*,' Final Technical Report, Grant No. AFOSR-87-0244, May, 1988.
2. Mihora, D.J., and P.J. Redmond, '*Electrostatically Formed Antennas*,' Journal of Spacecraft, Vol. 17, 465-473, 1980.
3. Lang, J.H., '*Electrostatically Figured Membrane Reflectors: An Overview*,' Large Space Systems Technology, NASA Conf. Pub 2269, Nov 30-Dec 2, 1982.
4. Alvarez, D.L., M. Dragovan, and G. Novak, '*Large Off-Axis Epoxy Paraboloids for Millimetric Telescopes and Optical Light Collectors*,' Reviews of Scientific Instruments 64, 261-262, 1993.

5. Borra, E.F., '*Liquid Mirrors*,' Canadian J. Physics, 73, (3-4) 1995.
6. Andersen, P.H., '*Will Future Astronomers Observe with Liquid Mirrors?*,' Phys Today, 40 (6), 1987.
7. Cardona-Nunez, O., A. Cornejo-Rodrigue, R. Diaz-Uribe, A. Cordero-Davila, J. Pedraza-Contreras, '*Comparison between toroidal and conic surfaces that best fit an off-axis conic section*,' Applied Optics, Vol. 26, No. 22, Nov. 1987.
8. Dragovan, M., '*Cutting surfaces of revolution for millimeter wave optics*,' Applied Optics, Vol 27, No. 19, October 1988.
9. Sagiv., A, '*Inflation of an Axisymmetric Membrane: Stress Analysis*,' Transactions of the ASME, Vol. 57, September 1990.
10. Roxburgh, D.G., '*Inflation of Nonlinearly Deformed Annular Elastic Membranes*,' Intl. Journal of Solids and Structures, Vol. 32, No. 14, pp 2041-2052, 1995.
11. Stevens, Jr., H.H., '*Behavior of Circular Membranes Stretched Above their Elastic Limit by Air Pressure*,' Experimental Stress Analysis, Vol. 2., pp-139-146, 1944.
12. Verron, E., G. Marckmann, B. Peseux, '*Dynamic inflation of non-linear elastic and viscoelastic rubber-like membranes*,' Intl. Journl for Numerical Methods on Engineering, 2001, 50:1233-1251.
13. Greschik, G., M. Mikulas, A. Palisoc., '*Approximations and Errors in Pressurized Axisymmetric Membrane Shape Predictions*,' AIAA A98-2101.
14. Greschik, G., A. Palisoc, C. Cassapakis, G. Veal, M. Mikulas, '*Approximating Paraboloids with Axisymmetric Pressurized Membranes*,' AIAA A98-2102.
15. Marker, D.K., J.M.Wilkes, R.A. Carreras, J.R.Rotge, C.H.Jenkins, J.T.Ash, '*Fundamentals of Membrane Optics*,' in Gossamer Spacecraft: Membrane and Inflatable Structures Technology for Space Applications, C.H.Jenkins, ed. AIAA Progress in Astronautics and Aeronautics Volume 191. 2001.